JOC The Journal of Organic Chemistry

pubs.acs.org/joc Note

A Method for Converting HPLC Peak Area from Online Reaction Monitoring to Concentration Using Nonlinear Regression

Madeleine C. Deem and Jason E. Hein*

Cite This: J. Org. Chem. 2023, 88, 1292−1297 Read Online

ACCESS | Metrics & More | Article Recommendations | Supporting Information

ABSTRACT: Online HPLC reaction progress monitoring provides detailed data-rich profiles; however, extracting kinetic information requires ultraviolet−visible response factors to determine concentrations from peak areas. If the reaction's overall mass balance is known and some analytical trend for all relevant species can be recorded, it is possible to estimate the absolute response factors of all species using a system of linear equations. We delineate a method using the Microsoft Solver plug-in to convert time course profiles to reagent concentrations without analytical standards.

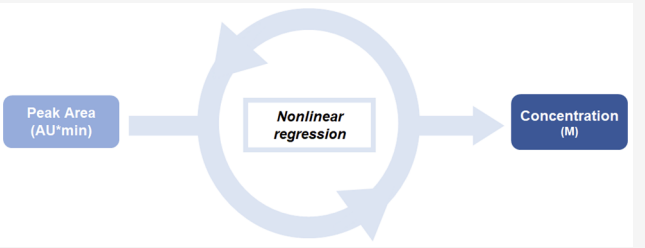

Time course reaction monitoring is an integral tool for understanding reactions.[1−3] Common analytical techniques in reaction monitoring include (U)HPLC-MS, GC-MS, FT-IR, Raman, and ^{1}H or ^{19}F NMR spectroscopy.[4,5] The primary data collected in time course reaction monitoring are generally peak areas versus time. In many cases, peak areas must be converted to concentration before meaningful conclusions and trends can be established.[2,3] The Beer−Lambert law describes the linear relationship between peak area and concentration.[6] This law can be used to convert peak areas measured by any spectrophotometer to concentration.[6] Peak area is divided by a molar absorptivity constant (ε) and by the path length of the detector (l) to calculate concentration (Figure 1).

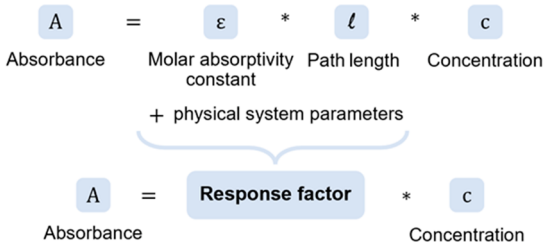

Figure 1. Depiction of the Beer−Lambert law and conversion between peak area and concentration using response factors.

The molar absorptivity constant, also known as the extinction coefficient, is unique to each chemical species.[6] The molar absorptivity constant, path length, and other physical parameters of the analytical instrument or sampling system can be combined into one general constant called the response factor.[7,8] Thus, if the response factor can be calculated, then peak area can be converted to concentration for that chemical species.

Calibration curves are a standard method for converting peak area to concentration.[7] While calibration curves are well-known and simple to understand, they are also time-consuming and require pure samples of all starting materials, intermediates, and side products or byproducts. Isolation of these species is often challenging. Variations in the experimental apparatus, such as modification of the HPLC stationary or mobile phase or degradation in detector performance over an experimental campaign, can render historical ex situ calibrations meaningless, forcing repetitive recalibration.[7] Any alteration of the reaction monitoring platform or analytical instrument requires a new set of calibration curves to be run.

The standard addition method is another method for determining response factors. This involves dosing known amounts of material into a reaction flask containing the other reagents and taking samples to determine the peak area at these known concentrations.[8] Unlike calibration curves, the standard addition method is accurate regardless of changes made to a system between experiments. However, both methods require access to pure material (starting materials, intermediates, side products or byproducts, and product). Quantitative NMR enables determination of response factors without pure standards. However, complex reaction mixtures with many chemically similar species may not have well-

Received: November 14, 2022
Published: January 10, 2023

https://doi.org/10.1021/acs.joc.2c02737
J. Org. Chem. 2023, 88, 1292−1297

resolved peaks, complicating integration and analysis via NMR.[9]

Nonlinear regressions can also be used to calculate response factors. This mathematical method for determining response factors is fast and does not require access to analytical standards. There are many nonlinear regression tools, including MATLAB, Mathematica, Python, and the Microsoft Excel Solver plugin. This paper describes the use of nonlinear regressions for determining concentration without experimental calibration. We will focus on the use of the Solver tool given the ubiquity and accessibility of Microsoft Excel. Our method has been validated by comparison of the concentrations calculated by the nonlinear regression method against the concentrations calculated by calibration curves.

WHAT IS THE SOLVER TOOL?

Solver is a nonlinear regression analysis tool in Microsoft Excel.[10−12] It employs the generalized reduced gradient (GRG) algorithm, which works via an iterative algorithm to change a set of defined parameters to minimize the residual sum of squares (eq 1).[10]

$$\text{residual sum of squares} = \sum (y_{\text{exp}} - y_{\text{calc}})^2 \quad (1)$$

Solver has been applied ubiquitously across the biological, pharmaceutical, and chemical sciences.[12−14] Solver is most frequently used as a nonlinear curve fitting tool.[10−17] Another less common application is the use of Solver to calculate response factors for multiple chemical species in a reaction system.[18] Several fundamental assumptions must be made when using nonlinear regressions to determine response factors. First, the complete mass balance must be known. All mass balance contributors must be identified, and there must be perfect mass balance for every sample. Second, each mass balance contributor must be able to be analyzed accurately (no peak overlap, good SNR, etc.). Finally, each chemical species must be within its linear range for the analytical instrument being used.

The use of Solver for calculating response factors has been previously reported.[18] However, no formal reports have validated the use of this non-experimental technique by comparing it to experimental data. Response factors can be determined according to the following steps.

(1) Set up a Microsoft Excel worksheet with peak area versus time data for each experiment.

(2) Define values for response factors. Set up a response factor cell for each chemical species, and input an arbitrary value for each response factor.

(3) Calculate concentration. Multiply the peak area of each chemical species by the corresponding response factor to calculate concentration. This will generate a data set with concentration versus time values for each experiment.

(4) Calculate the mass balance at each time point. Sum the calculated concentration for each chemical species that contributes to the mass balance. The stoichiometry of each chemical species in the mass balance equation must be considered.

(5) Calculate the mass balance error at each time point. There are multiple methods for determining error, the most common of which is to calculate the residual sum of squares. Alternatively, the absolute value of the difference between the theoretical and expected mass balances at each time point can be calculated.

(6) Calculate the mass balance error for the entire data set. Sum the mass balance errors at each time point for the entire excel sheet.

The Excel sheet after steps 1−6 should resemble Figure 2.

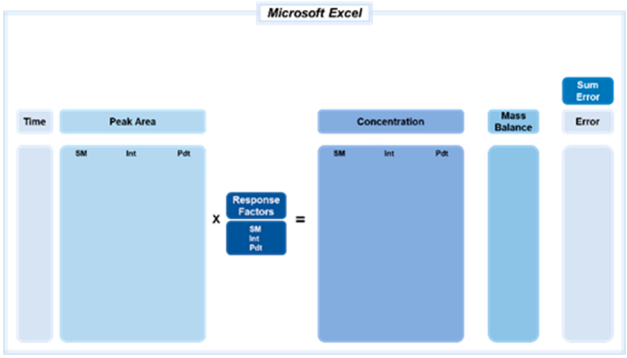

Figure 2. Depiction of how to organize data in a Microsoft Excel sheet to calculate concentrations using the Solver tool.

(7) Run the Solver tool. Set the target cell as the sum of all mass balance errors; set the variable cells as the response factors, and set the objective to minimize. An example setup is depicted in Figure 3. Solver will find the set of response factors that give the mass balances closest to the theoretical mass balance.

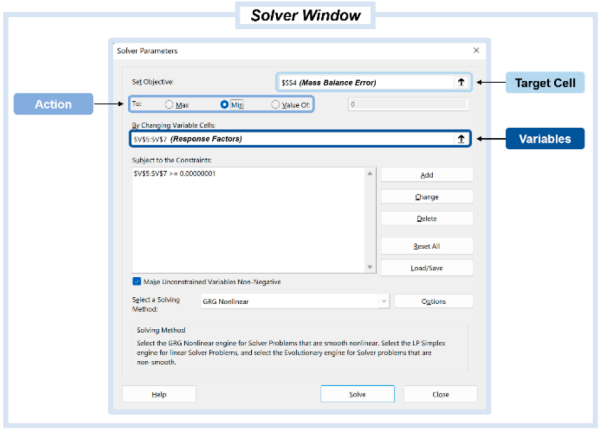

Figure 3. Example of how to set up the Solver tool in Microsoft Excel.

(8) Run Solver again. The "multistart" option should also be enabled in the Solver window, which changes the arbitrary starting values input for the response factors and ensures that Solver arrives at the same values regardless of the starting point. It is also necessary to run Solver multiple times to ensure that the universal, rather than a local, minimum has been found.

Case Study 1: Simple Reaction System without Intermediates. The time course reaction profile of the epoxidation of *trans*-stilbene (**1**) with *m*CPBA was recorded via a previously described automated sampling platform[19] coupled with online HPLC-MS. The peak area versus time trends of the conversion of **1** to 2,3-diphenyloxirane (**2**) were first converted to concentration using a set of calibration curves (Figure 4, filled circles). The same data were then converted to concentration via the nonlinear regression method (Figure 4, empty circles). In this method, the peak

https://doi.org/10.1021/acs.joc.2c02737
J. Org. Chem. 2023, 88, 1292−1297

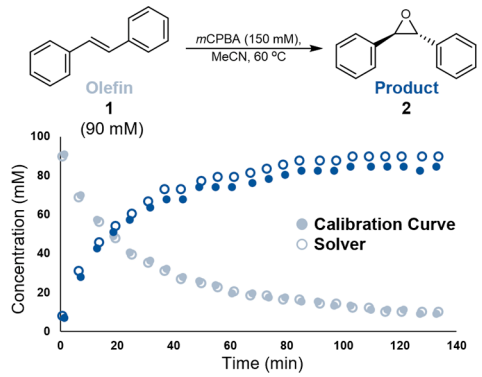

Figure 4. Overlay of the concentration vs time profile of a simple *m*CPBA epoxidation reaction solved for via two methods. Empty circles represent concentration data from the nonlinear regression method, and filled circles represent calibration curve concentrations.

area versus time trends were converted to concentration using the procedure described in the previous section. The Solver tool was run with the objective to minimize the error in mass balance by changing the response factor values (Figure 3). Though not identical, the concentration values determined by each method are very similar. For the purposes of a kinetic study that requires an overlay of reaction profiles under several different initial concentrations, these data sets would lead to the same conclusions, and therefore, the Solver method is a valid way to calculate concentration.

Case Study 2: Simple Reaction System with One Intermediate. Another simple system was studied to further validate the accuracy of the Solver-based method. The time course reaction profile of the Buchwald Hartwig amination between 2,7-dibromo-9,9-dimethyl-9*H*-fluorene (**3**) and 4,4′-dimethoxydiphenylamine (**4**) was recorded. The time course data show the formation of the monoaminated intermediate (**5**) before the diaminated product (**6**) (Figure 5). The time course reaction profile of this reaction has been previously reported, but the treatment of the data is novel.[20]

The peak area trends were again converted to concentration by two methods: calibration curves and the Solver-based method. The overlay of concentration versus time profiles as determined by calibration curves and Solver is shown in Figure 5. The agreement between the two trends is excellent, and the calibration curve and Solver mass balances are well matched (Figure S18). These data demonstrate the accuracy of using the Solver tool to calculate response factors.

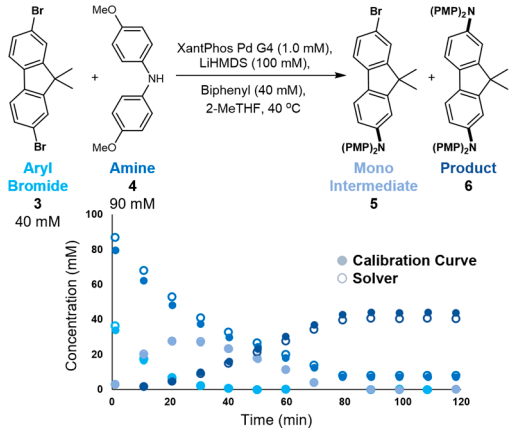

Figure 5. Concentration vs time reaction profile of the amination of **3** and **4**. Concentration units have been solved for using two methods. Filled circles reflect the Solver method, and empty circles represent the calibration curve.

Case Study 3: Complex Reaction with Many Intermediates. Time course data of the Buchwald Hartwig amination of a more complex tetrabrominated arene (**7**) were gathered. The time course reaction profile shows the formation of a tetraaminated product preceded by four intermediates: a monoaminated intermediate, two diaminated regioisomers, and a triaminated intermediate (Figure 6). The mass balance was calculated, and the Solver tool was used to calculate the concentration of each species.

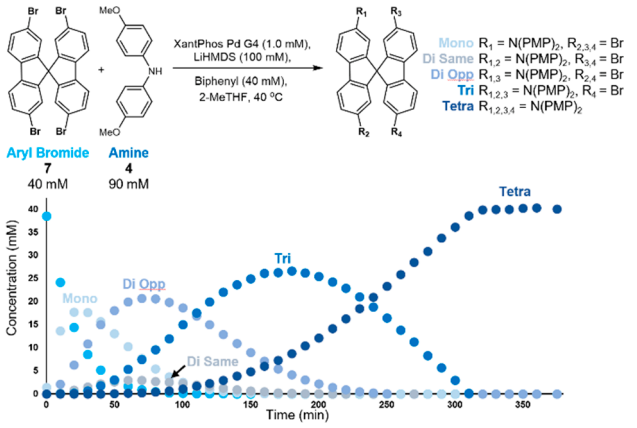

Figure 6. Temporal concentration profile of the Buchwald Hartwig amination of 7. Concentrations were calculated using the Solver method.

Using the Solver method to determine concentration for this reaction prevented a difficult isolation of several intermediates and a side product. This example demonstrates the utility of using the nonlinear regression method over traditional experimental calibration methods.

Case Study 4: Limitations of the Nonlinear Regression Method. Though the nonlinear regression method is convenient and conserves material, as exemplified in the examples presented above, there are limitations to its use. It cannot be used if there are unidentified peaks or unknown species in the mass balance. This method also cannot be used if one of the chemical species is outside of its linear range. Cases in which nonlinear regressions cannot be used are identified by looking at the mass balance of the reaction. If the mass balance is nonconstant, is significantly off in the first or last time points, or is not at the correct value, nonlinear regression is likely not an appropriate method.

A simple Sonogashira coupling between iodobenzene (**8**) and phenylacetylene (**9**) was studied. When the data were converted to concentration via Solver, there were obvious issues with the mass balance (Figure 7). The mass balance trend was nonconstant and did not match the expected theoretical value. A set of calibration curves were run and revealed that the concentrations of diphenylacetylene (**10**) were outside the linear range of the material (Figure 7). The incompatibility of a nonlinear regression method was quickly identified in this case by plotting the mass balance. It is necessary to check the linearity and constancy of the mass balance early in the time course data collection process.

https://doi.org/10.1021/acs.joc.2c02737
J. Org. Chem. 2023, 88, 1292−1297

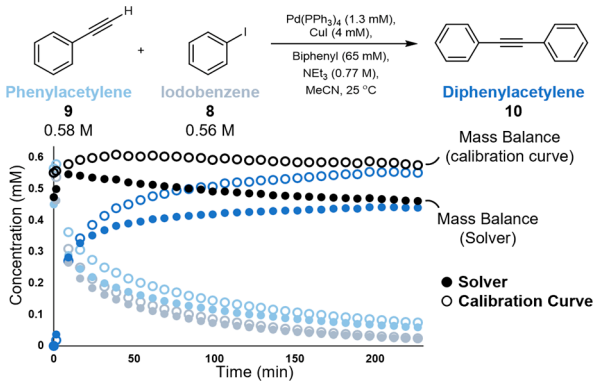

Figure 7. Overlay of concentration vs time profiles of a Sonogashira reaction. Concentration calculated accurately with a calibration curve and inaccurately with the Solver method.

Case Study 5: Incomplete Mass Balance Precludes the Use of the Nonlinear Regression Method. The dihydroxylation of methyl *trans*-cinnamate (**11**) using catalytic osmium and a chiral cinchona alkaloid ligand was monitored (Figure 8). The experimental mass balance was nonconstant

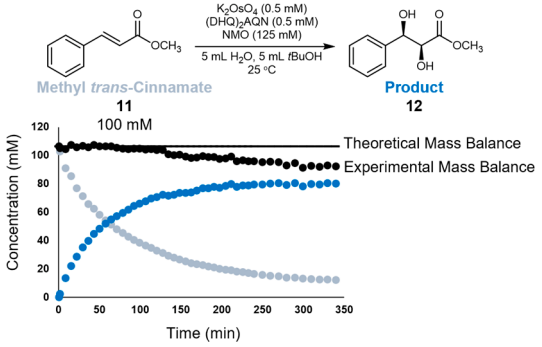

Figure 8. Concentration vs time profile of the sharpless asymmetric dihydroxylation of **11**. Concentrations calculated using calibration curves. The nonconstant experimental mass balance trend was due to product degradation.

due to degradation of the product, methyl-2,3-dihydroxy-3-phenylproanoate (**12**), under reaction conditions. The product degradation side product was never identified, and the full mass balance equation was not known. Thus, the Solver-based method could not be applied to these data. The concentration versus time trends shown in Figure 8 were calculated using calibration curves. The mass balance versus time trend is a quick and simple metric to gauge the applicability of the nonlinear regression method for a data set.

We have provided instructions and experimental validation for the use of the Excel Solver tool for calculating response factors. Experimental calibration methods, such as calibration curves and standard additions, require access to isolated pure materials, which can be challenging and time-consuming. Variations in experimental apparatus require the determination of new response factors, which would require additional material and time if calibration curves were employed. Conversely, it is facile to solve for multiple sets of response factors in a data set using the nonlinear regression method (page S15 of the Supporting Information). This method cannot be applied ubiquitously, but cases in which the nonlinear regression method cannot be used are readily identified by examining the mass balance versus time trend. We feel this is an underused method and is practical for many disciplines that require access to temporal concentration data.

EXPERIMENTAL SECTION

General Information. All chemicals were purchased from AK Scientific, Ambeed, Combi-Blocks, Millipore Sigma, Oakwood Chemicals, or Strem Chemicals and used without further purification. THF was purchased from Fischer Scientific and dispensed from an MBraun solvent purification system. ^{1}H and ^{13}C{1H} NMR spectra were recorded on a Bruker AV-400 MHz spectrometer and were referenced to the residual solvent peaks (THF-d_8 1.72 and 3.58 ppm for ^{1}H NMR and 25.3 and 67.2 ppm for ^{13}C{^{1}H} NMR; DMSO-d_6 2.50 ppm for ^{1}H NMR and 39.5 ppm for ^{13}C{^{1}H} NMR). ^{1}H NMR multiplicity was reported using the following abbreviations: br, broad; s, singlet; d, doublet; t, triplet; q, quartet; quint, quintet; sext, sextuplet; sept, septuplet; m, multiplet. Integration values and coupling constants were reported in hertz. Analysis via HPLC-MS was conducted using an Agilent 1200 HPLC instrument equipped with an Agilent model G1379B degasser, a model G1312A binary pump, a model G1316A thermal column compartment, a diode array detector, and a model 6120 single quad mass spectrometer. Data processing was done using ChemStation (Agilent) and another proprietary third-party software. Time course reaction profiles were recorded via online *ex situ* HPLC-MS analysis. An automated sampling platform was used to take reaction samples and deliver them to the HPLC-MS instrument. A depiction of the automated sampling platform is shown in Figure S1.

Experimental Information. *2,3-Diphenyloxirane (**2**).* To a 15 mL two-neck round-bottom flask with a stir bar were added methyl *trans*-stilbene (0.901 g, 5.0 mmol), 50 mL of DCM, and *m*CPBA (1.294 g, 7.5 mmol). The reaction mixture was stirred at 30 °C in an EasyMax 102 Thermostat system for 12 h. The reaction mixture was cooled to room temperature, and the precipitate was filtered. The organic phase was extracted with 3 × 10 mL of saturated sodium thiosulfate, 3 × 10 mL of saturated sodium bicarbonate, and 1 × 10 mL of brine. The combined organic layers were dried over $MgSO_4$, filtered, and concentrated *in vacuo*. The crude 2,3-diphenyloxirane (0.902 g, 4.6 mmol, 92%) was not purified further. Characterization is consistent with that in the literature.[211] ^{1}H NMR (400 MHz, $CDCl_3$): δ 7.43−7.31 (m, 10H), 3.88 (s, 2H). ^{13}C{^{1}H} NMR (101 MHz, $CDCl_3$): δ 137.3, 128.7, 128.5, 125.6, 63.0.

*7-Bromo-N,N-bis(4-methoxyphenyl)-9,9-dimethyl-9H-fluoren-2-amine (**5**).* To an oven-dried 4 dram vial with a stir bar were added 4,4′-dimethoxydiphenylamine (218 mg, 0.95 mmol), 2,7-dibromo-9,9-dimethyl-9*H*-fluorene (352 mg, 1.00 mmol), and XantPhos Pd G4 (24 mg, 0.025 mmol). The vial was sealed with a septum cap and placed in a glovebox. LiHMDS (189 mg, 1.13 mmol) was added to the reaction vial. The vial was removed from the glovebox and placed under Ar on a Schlenk line. Ten milliliters of 2-MeTHF was added, and the reaction mixture was stirred at 40 °C in an EasyMax 102 Thermostat system for 16 h. The reaction mixture was cooled to room temperature and poured into a separatory funnel containing 10 mL of saturated aqueous ammonium chloride. The aqueous layer was extracted with 3 × 10 mL of ethyl acetate, and the combined organic layers were extracted with 1 × 10 mL of brine. The combined organic layers were dried over $MgSO_4$, filtered, and concentrated *in vacuo*. The crude reaction mixture was purified via flash chromatography using a Buchi autocolumn. A reverse phase C18 column was used with an isocratic solvent mixture of 40% acetonitrile in water (0.1% formic acid modified) to afford the product (380 mg, 0.76 mmol, 76%). Characterization is consistent with that in the literature.[201] ^{1}H NMR (400 MHz, THF): δ 7.58−7.46 (m, 3H), 7.39 (dd, J = 8.1, 1.8 Hz, 1H), 7.04 (dd, J = 9.2, 2.1 Hz, 5H), 6.88−6.80 (m, 5H), 3.76 (s, 6H), 1.36 (s, 6H). ^{13}C{^{1}H} NMR (101 MHz, THF): δ 157.2, 156.6, 155.6, 150.1, 142.1, 139.6, 131.7, 130.8, 127.3, 126.8, 121.5, 121.29, 120.9, 120.2, 115.7, 115.5, 55.6, 47.8, 27.2.

*N2,N2,N7,N7-Tetrakis(4-methoxyphenyl)-9,9-dimethyl-9H-fluorene-2,7-diamine (**6**).* To an oven-dried 4 dram vial with a stir bar

https://doi.org/10.1021/acs.joc.2c02737
J. Org. Chem. 2023, 88, 1292−1297

were added 4,4′-dimethoxydiphenylamine (206 mg, 0.9 mmol), 2,7-dibromo-9,9-dimethyl-9*H*-fluorene (141 mg, 0.4 mmol), and XantPhos Pd G4 (10 mg, 0.01 mmol). The vial was sealed with a septum cap and placed in a glovebox. LiHMDS (167 mg, 1.0 mmol) was added to the reaction vial. The vial was removed from the glovebox and placed under Ar on a Schlenk line. Ten milliliters of 2-MeTHF was added, and the reaction mixture stirred at 40 °C in an EasyMax 102 Thermostat system for 16 h. The reaction mixture was cooled to room temperature and poured into a separatory funnel containing 10 mL of saturated aqueous ammonium chloride. The aqueous layer was extracted with 3 × 10 mL of ethyl acetate, and the combined organic layers were extracted with 1 × 10 mL of brine. The combined organic layers were dried over $MgSO_4$, filtered, and concentrated *in vacuo*. The crude reaction mixture was purified via trituration. One milliliter of THF was used to dissolve the crude solid, and 25 mL of methanol was added slowly to the reaction flask causing the solid to precipitate. The precipitate was collected via suction filtration to afford the product (224 mg, 0.34 mmol, 86%). Characterization is consistent with that in the literature.[201] ^{1}H NMR (400 MHz, THF): δ 7.39 (d, J = 8.3 Hz, 3H), 7.03 (d, J = 9.0 Hz, 8H), 6.82 (d, J = 9.0 Hz, 8H), 3.74 (s, 16H), 1.28 (s, 6H). ^{13}C{^{1}H} NMR (101 MHz, THF): δ 156.9, 155.5, 148.5, 142.5, 133.5, 126.9, 121.3, 120.3, 116.5, 115.4, 55.6, 47.3, 27.5.

*1,2-Diphenylethyne (**10**).* To an oven-dried 10 mL three-neck round-bottom flask was added biphenyl (77 mg, 0.5 mmol). The flask was evacuated and backfilled with Ar thrice. Under positive pressure, the EasySampler probe was inserted into the reaction flask. Then, 12.0 mL of dry acetonitrile, iodobenzene (0.89 mL, 8.0 mmol), phenylacetylene (0.97 mL, 8.8 mmol), and triethylamine (1.67 mL, 12.0 mmol) were added to the reaction flask. The reaction was initiated by the addition of CuI (11.4 mg, 0.06 mmol) and $Pd(PPh_3)_4$ (23.1 mg, 0.02 mmol). The reaction mixture was stirred at 25 °C and sampled every 8 min for 3.5 h. The reaction mixture was poured into a separatory funnel containing saturated aqueous ammonium chloride and extracted with 3 × 10 mL of DCM. The combined organic layers were extracted with 1 × 10 mL of brine. The organic layers were dried over $MgSO_4$, filtered, and concentrated *in vacuo* to afford the crude diphenylacetylene product (549.5 mg, 3.1 mmol, 98%). No further purification was necessary. Characterization is consistent with that in the literature.[221] ^{1}H NMR (400 MHz, $CDCl_3$): δ 7.78−7.55 (m, 4H), 7.39 (dd, J = 5.6, 1.8 Hz, 6H). ^{13}C{^{1}H} NMR (101 MHz, $CDCl_3$): δ 131.7, 128.5, 128.4, 123.4, 89.5.

*Methyl-2,3-dihydroxy-3-phenylproanoate (**12**).* A catalyst solution was made by dissolving potassium osmate dihydrate (10 mg, 0.02 mmol) in 2.2 mL of water. A ligand stock solution was made by dissolving hydroquinine anthraquinone-1,4-diyl diether (20 mg, 0.02 mmol) in 2.3 mL of *tert*-butanol. To a 15 mL two-neck round-bottom flask with a stir bar were added methyl *trans*-cinnamate (162 mg, 1.0 mmol), 4.5 mL of *tert*-butanol, 4.5 mL of water, 0.5 mL of the catalyst solution, and 0.5 mL of the ligand solution. The reaction was initiated via addition of *N*-methylmorpholine oxide (146 mg, 1.25 mmol). The reaction mixture was stirred at 25 °C for 4 h. The reaction mixture was partitioned in a separatory funnel containing 10 mL of saturated aqueous ammonium chloride and 10 mL of ethyl acetate. The reaction mixture was extracted with 3 × 10 mL of saturated sodium thiosulfate. The combined organic layers were extracted with 10 mL of brine, dried over $MgSO_4$, filtered, and concentrated *in vacuo*. The crude methyl-2,3-dihydroxy-3-phenylproanoate (169 mg, 0.86 mmol, 86%) was not purified further. Characterization is consistent with that in the literature.[231] ^{1}H NMR (400 MHz, DMSO): δ 7.40−7.27 (m, 4H), 7.27−7.19 (m, 1H), 5.50 (d, J = 5.9 Hz, 1H), 5.33 (d, J = 7.4 Hz, 1H), 4.85 (dd, J = 5.9, 3.9 Hz, 1H), 4.16 (dd, J = 7.4, 3.9 Hz, 1H), 3.59 (s, 3H). ^{13}C{^{1}H} NMR (101 MHz, DMSO): δ 172.7, 142.0, 127.7, 127.0, 126.7, 75.6, 74.1, 51.4.

■ ASSOCIATED CONTENT

Data Availability Statement

The data underlying this study are available in the published article and its Supporting Information.

Supporting Information

The Supporting Information is available free of charge at https://pubs.acs.org/doi/10.1021/acs.joc.2c02737.

Details of the Solver method and experimental procedures (PDF)

■ AUTHOR INFORMATION

Corresponding Author

Jason E. Hein − *Department of Chemistry, University of British Columbia, Vancouver, British Columbia V6T 1Z1, Canada;* orcid.org/0000-0002-4345-3005; Email: jhein@chem.ubc.ca

Author

Madeleine C. Deem − *Department of Chemistry, University of British Columbia, Vancouver, British Columbia V6T 1Z1, Canada*

Complete contact information is available at: https://pubs.acs.org/10.1021/acs.joc.2c02737

Notes

The authors declare no competing financial interest.

■ ACKNOWLEDGMENTS

The authors gratefully acknowledge Mettler-Toledo Autochem for their generous donation of process analytical equipment (Easy Max 102). The authors also thank Dr. Josh Derasp for critical advice and guidance during the preparation of the manuscript.

■ REFERENCES

(1) Blackmond, D. G. Reaction Progress Kinetic Analysis: A Powerful Methodology for Mechanistic Studies of Complex Catalytic Reactions. *Angew. Chem., Int. Ed.* **2005**, *44* (28), 4302−4320.

(2) Bures, J. A Simple Graphical Method to Determine the Order in Catalyst. *Angew. Chem., Int. Ed.* **2016**, *55* (6), 2028−2031.

(3) Bures, J. Variable Time Normalization Analysis: General Graphical Elucidation of Reaction Orders from Concentration Profiles. *Angew. Chem., Int. Ed.* **2016**, *55* (52), 16084−16087.

(4) Nielsen, C. D. T.; Bures, J. Visual kinetic analysis. *Chem. Sci.* **2019**, *10*, 348−353.

(5) Kukor, A. J.; Guy, M. A.; Hawkins, J. M.; Hein, J. E. A robust new tool for online solution-phase sampling of crystallizations. *React. Chem. & Eng.* **2021**, *6* (11), 2042−2049.

(6) Mayerhöfer, T. G.; Pahlow, S.; Popp, J. The Bouguer-Beer-Lambert Law: Shining Light on the Obscure. *ChemPhysChem* **2020**, *21* (18), 2029−2046.

(7) Harris, D. C. H.*Exploring Chemical Analysis*, 5th ed.; W. H. Freeman, 2012.

(8) Hutchinson, G.; Welsh, C. D. M.; Bures, J. Use of Standard Addition to Quantify In Situ FTIR Reaction Data. *J. Org. Chem.* **2021**, *86*, 2012−2016.

(9) Ben-Tal, Y.; Boaler, P. J.; Dale, H. J. A.; Dooley, R. E.; Fohn, N. A.; Gao, Y.; Garcia-Dominguez, A.; Grant, K. M.; Hall, A. M.R.; Hayes, H. L. D.; Kucharski, M. M.; Wei, R.; Lloyd-Jones, G. C. Mechanistic analysis by NMR spectroscopy: A users guide. *Prog. Nucl. Magn. Reson. Spectrosc.* **2022**, *129*, 28−106.

(10) Harris, D. C. Nonlinear Least-Squares Curve Fitting with Microsoft Excel Solver. *J. Chem. Educ.* **1998**, *75* (1), 119−121.

(11) Hu, W.; Xie, J.; Chau, H. W.; Si, B. C. Evaluation of parameter uncertainties in nonlinear regression using Microsoft Excel Spreadsheet. *Environ. Syst. Res.* **2015**, *4*, 4.

(12) Brown, A. M. A step-by-step guide to non-linear regression analysis of experimental data using a Microsoft Excel spreadsheet. *Comput. Methods Programs Biomed* **2001**, *65*, 191−200.

(13) Dias, A. A.; Pinto, P. A.; Fraga, I.; Bezerra, R. M. F. Diagnosis of Enzyme Inhibition Using Excel Solver: A Combined Dry and Wet Laboratory Exercise. *J. Chem. Educ.* **2014**, *91*, 1017−1021.
(14) Bowen, W. P.; Jerman, J. C. Nonlinear regression using spreadsheets. *TiPS* **1995**, *16*, 413−417.
(15) Copeland, T. G. The use of non-linear least squares analysis. *J. Chem. Educ.* **1984**, *61* (9), 778−779.
(16) Denton, P. Analysis of First-Order Kinetics Using Microsoft Excel Solver. *J. Chem. Educ.* **2000**, *77* (11), 1524−1525.
(17) Muelleman, A. W.; Glaser, R. E. Learning To Read Spectra: Teaching Decomposition with Excel in a Scientific Writing Course. *J. Chem. Educ.* **2018**, *95* (3), 476−481.
(18) Billo, J. E.*Excel for Chemists*, 2nd ed.; Wiley-VCH, 2001.
(19) Malig, T. C.; Yunker, L. P. E.; Steiner, S.; Hein, J. E. Using an Automated Monitoring Platform for Investigations of Biphasic Reactions. *ACS Catal.* **2020**, *10* (22), 13236−13244.
(20) Deem, M. C.; Derasp, J. S.; Malig, T. C.; Legard, K.; Berlinguette, C. P.; Hein, J. E. Ring walking as a regioselectivity control element in Pd-catalyzed C-N cross-coupling. *Nat. Commun.* **2022**, *13*, 2869.
(21) Lusinchi, X.; Hanquet, G. Oxygen transfer reactions from an oxaziridinium tetrafluoroborate salt to olefins. *Tetrahedron* **1997**, *53* (40), 13727−13738.
(22) Ma, J.; Li, G.; Qiao, Y.; Tu, J.; Liu, S.; Xu, F. Palladium-Catalyzed Annulation of 2,2′-Dibromobiphenyls with Alkynes: Synthesis of Functionalized Phenanthrenes and Dibenzochrysenes. *Synlett* **2015**, *26* (14), 1991−1996.
(23) Wang, Z.; Kolb, H. C.; Sharpless, K. B. Large-Scale and Highly Enantioselective Synthesis of the Taxol C-13 Side Chain through Asymmetric Dihydroxylation. *J. Org. Chem.* **1994**, *59* (17), 5104−5105.

https://doi.org/10.1021/acs.joc.2c02737
J. Org. Chem. 2023, 88, 1292−1297